Research Square

Preprints are preliminary reports that have not undergone peer review.
They should not be considered conclusive, used to inform clinical practice,
or referenced by the media as validated information.

The Influence of Structural Changes in phosphonamide Flame Retardant on the Properties of Thermoplastic Polyurethane Elastomers

Kai Wei
Yingxin Li
Yajun Chen
chenyajun@th.btbu.edu.cn

Beijing Technology and Business University - Fucheng Road Campus https://orcid.org/0000-0002-3082-2078

Research Article

Keywords: phosphoramidate flame retardants, thermoplastic polyurethane, terminal group

Posted Date: May 27th, 2026

DOI: https://doi.org/10.21203/rs.3.rs-9624196/v1

License: This work is licensed under a Creative Commons Attribution 4.0 International License.
Read Full License

Version of Record: A version of this preprint was published at Journal of Polymer Research on September 26th, 2026. See the published version at https://doi.org/10.1007/s10965-026-05132-w.

Abstract

This study involved the synthesis of three novel phosphonamide flame retardants, each featuring a distinct terminal group: amino-terminated PPDA, phenyl-terminated DAPPO, and thiazole-terminated PPNDB. The flame retardancy and mechanical properties of these three phosphonamide flame retardants in TPU were compared, aiming to explore an efficient flame retardant TPU system. Among the synthesized flame retardants, PPDA showed superior flame retardancy in TPU. At equal loading, the limiting oxygen index of TPU/PPDA was higher than that of TPU/DAPPO. Dropping of the TPU composite was suppressed only when 12 wt% PPDA was added. At a 9 wt% loading, the TPU/PPDA composite exhibited a 58% lower the peak heat release rate than pure TPU, outperforming composites with DAPPO or PPNDB at the same concentration. The results from TG, XPS, and SEM of the residual char indicate that a stable three-dimensional cross-linked network structure is formed in TPU by PPDA. Among the three flame retardants, PPDA has the smallest influence on the mechanical properties of the TPU composite. This study is considered to provide a new approach for halogen-free flame retardant TPU.

1. Introduction

Thermoplastic polyurethane elastomer (TPU) is a polymer material known for its high performance, distinguished by outstanding wear resistance, substantial oil resistance, and elevated modulus. This material finds extensive application across various sectors, including the electrical industry, sports equipment, automotive components, and construction materials [1–8]. Nevertheless, untreated TPU poses a significant fire hazard, exhibiting a limiting oxygen index (LOI) of approximately 20%. Additionally, its combustion releases substantial amounts of toxic smoke, which greatly limits its usability in numerous areas. Therefore, there is a strong demand for flame retardant treatment of TPU [6–11].

The flame retardancy of thermoplastic polyurethane is achieved through two principal approaches: intrinsic and additive [12], with mono-component organic flame retardants, as a class of additive flame retardants, having attracted considerable research interest in recent years [13].

Organic flame retardants comprise compounds that contain flame-retardant elements, including P, N, Si and S. A key advantage of organic flame retardants over their inorganic counterparts is their ease of molecular design, allowing for the integration of multiple flame retardant elements into a single, multifunctional molecule [13]. Organophosphorus and organophosphorus-nitrogen flame retardants are commonly utilized because of their effective flame retardant properties and favorable compatibility with TPU [14–17]. Li et al. utilized dipyromellitic diimide (DMPY) as an effective flame retardant additive in TPU. The addition of 15 wt% of DMPY successfully allowed the composite to attain a UL 94 V-0 classification. Moreover, this classification was maintained even after prolonged exposure to water at 70°C for a duration of 168 hours without sacrificing mechanical performance. [18]. Hao et al. developed a phosphorus-containing Schiff-base derivative (SAME). At a remarkably low loading of 4 wt%, it imparts exceptional flame retardancy to TPU, evidenced by a UL 94 V-0 rating and an LOI greater than 30%. Its

dominant mode of action is gas-phase flame inhibition [19, 20]. These results underscore the high efficiency of phosphorous-nitrogen flame retardants and demonstrate a pronounced phosphorus–nitrogen synergistic effect [7].

Phosphoramides are also classified as phosphorus–nitrogen single-component organic flame retardants. In recent years, they have been applied to flame retard TPU, and good performance has been achieved. Typical examples are PPBPP, DCPCD, and POP [21, 22]. Chen et al. prepared a piperazine-based compound (PPBPP); addition of 3.0 wt % PPBPP sufficed for UL 94 V-0, while raising the content to 12.0 wt % eliminated melt dripping. Concurrently, mechanical properties were gradually restored as the PPBPP fraction increased [23]. Li et al. developed a new flame retardant known as DCPCD, which features phosphonamide bonds. By incorporating 12 wt% of DCPCD, the LOI for the TPU composite increased to 30.8%, resulting in a UL 94 V-0 classification. Moreover, the peak heat release rate (PHRR) for the TPU composite experienced a significant reduction of 67.7% [24]. Shi et al. reported that a 30% loading of the polymeric flame retardant POP in TPU yielded an LOI of 29.2% and a UL 94 V-0 rating, with minimal impact on mechanical properties and transparency owing to their excellent compatibility between TPU and POP [25].

In this paper, we designed and synthesized three structurally different phosphonamide flame retardants (designated as PPDA, DAPPO, and PPNDB) to explore the effects of changes in the terminal group structure on the flame retardant and mechanical properties of TPU when using phosphonamide molecules as flame retardants. By analyzing combustion behavior, evaluating thermal stability, and conducting mechanical property tests, this study investigates how the changes in the terminal group structure of flame retardants affect the evolution of the condensed-phase char layer and interfacial compatibility. It clarifies the differences in flame retardancy of phosphonamide flame retardants with distinct structures. This research provides insights into the rational design of phosphonamide flame retardants and offers a new approach for halogen-free flame retardant TPU.

2. Experimental section

2.1 Materials

The materials and reagents used in the experiments were as follows: Phenylphosphonyl dichloride (AR, 99%, Macklin), p-phenylenediamine(AR, 99%, J&K Scientific), dichloroethane(AR, 99.5%, Macklin), aniline(AR, 99.5%, Macklin), 2-aminobenzothiazole(AR, Macklin),Triethylamine(AR, 99%, Macklin), Tetrahydrofuran(AR, 98%, Titan), Thermoplastic polyurethane elastomer(TPU, 9380A, Bayer Company), Distilled water(Laboratory).

2.2 Synthesis of the PPDA

Initially, p-phenylenediamine (10.8 g, 0.10 mol) was charged to a 250 mL four-necked round-bottom flask, followed sequentially by triethylamine (14 ml, 0.10 mol) and anhydrous THF (100 ml). Add phenylphosphonyl dichloride (9.7 g, 0.05 mol) and tetrahydrofuran (30 ml) to a constant pressure

dropping funnel. The mixture in the funnel is added dropwise into the flask over one hour while maintaining the temperature at 0–5℃. Following the addition, the reaction proceeded at room temperature for 1 hour, followed by an additional 8 hours while maintaining the temperature below 20°C. Following 24-hour standing, the mixture was suction-filtered, and the collected solid was washed with distilled water followed by 80°C hot water. The resulting material was then dried in a vacuum oven at 90°C for 6 hours, yielding a light purple solid.

2.3 Synthesis of the DAPPO

First, add tetrahydrofuran (200 ml), triethylamine (28 ml, 0.2 mol), and aniline (120 ml, 0.2 mol) to a four-neck flask equipped with a thermometer, a stirrer, a constant pressure dropping funnel, and a reflux condenser. Then, dissolve phenylphosphonyl dichloride (19.5 g, 0.1 mol) in tetrahydrofuran (50 ml) and add the solution to the constant pressure dropping funnel. Under the condition of an ice-water bath (0–5℃), the solution in the funnel is added dropwise slowly (2–4 hours). After the addition is complete, the temperature is raised to 20℃ and the reaction is continued for 8 hours. After the reaction is over, the mixture is filtered by vacuum pump to separate the solid and liquid phases. The resulting solid is washed repeatedly with distilled water several times and then dried under vacuum to obtain a white powder.

2.4 Synthesis of the PPNDB

A solution was first prepared by dissolving 2-aminobenzothiazole (15.0 g, 0.1 mol) and triethylamine (41.4 ml, 0.3 mol) in dichloroethane (60 ml), which was then transferred to a 250 ml three-neck reactor equipped with a mechanical stirrer, temperature sensor, constant pressure dropping funnel. The reaction system was precisely controlled at 0–5℃ by an ice bath. Under continuous stirring, a mixture of phenylphosphonyl dichloride (9.8 g, 0.045 mol) and dichloroethane (50 ml) was added dropwise at a rate of 0.5 ml/min over 2 hours. After adding the necessary components, the ice bath was taken away, and the mixture was heated to 84°C while being refluxed for 8 hours with constant stirring. After cooling to 25°C, vacuum filtration was employed to collect the resulting precipitate. The solid was subsequently washed with deionized water and subjected to drying in a vacuum at 80°C for 8 hours, yielding a pale yellow crystalline solid as the final product. Scheme 1 illustrates the synthetic pathways for PPDA, DAPPO, and PPNDB.

2.5 Preparation of flame retardant TPU Materials

Flame retardant TPU composites were prepared by melt blending process. The specific formulation is shown in Table 1. The processing was carried out using a torque rheometer with the process parameters set at a mixing temperature of 180℃, rotor speed of 60 rpm, and mixing time of 10 minutes. The blended products were then hot-pressed into standard sheets (thickness of 3.0 ± 0.1 mm and 2.0 ± 0.1 mm, the holding time is 5min) with a hot press at 180℃ and 10 MPa pressure. Subsequently, the sheets were processed into standard test specimens of various shapes using a standard specimen die-cutter.

Table 1
Formulations for flame retardant TPU composites with PPDA, DAPPO, and PPNDB.

Sample	TPU(g)	PPDA(g)	DAPPO(g)	PPNDB(g)
TPU	200	0.0	0.0	0.0
TPU/PPDA-3	194	6.0	0.0	0.0
TPU/PPDA-6	188	12.0	0.0	0.0
TPU/PPDA-9	182	18.0	0.0	0.0
TPU/PPDA-12	176	24.0	0.0	0.0
TPU/DAPPO-3	194	0.0	6.0	0.0
TPU/DAPPO-6	188	0.0	12.0	0.0
TPU/DAPPO-9	182	0.0	18.0	0.0
TPU/DAPPO-12	176	0.0	24.0	0.0
TPU/PPNDB-3	194	0.0	0.0	6.0
TPUPPNDB-6	188	0.0	0.0	12.0
TPU/PPNDB-9	182	0.0	0.0	18.0
TPU/PPNDB-12	176	0.0	0.0	24.0

2.6 Characterization

The characterization of the structure of the flame retardant included methods like Fourier-transform infrared spectroscopy (FT-IR, Thermo iN10MX) and nuclear magnetic resonance spectroscopy (NMR, Bruker AVANCE III HD, Germany). For FTIR analysis, the spectrum was captured by performing 32 scans across a range of 500–4000 cm^{-1}. The ^1H NMR measurements were conducted using a 700 MHz instrument with DMSO-d_6 acting as the solvent.

Thermogravimetric (TG, PerkinElmer STA 8000, USA) analysis was utilized to assess the thermal characteristics of both the flame retardant and its composites. The experiments were carried out in a nitrogen-purged furnace, where the samples were subjected to a heating process that gradually increased their temperature from 50 to 700°C. This temperature elevation occurred at a steady rate of 20°C per minute.

To evaluate the flame retardancy, tests were conducted using the limiting oxygen index (LOI, Concept Equipment Ltd. 300,800, UK), vertical burning (UL 94, FTT 0082, UK), and cone calorimetry (CCT, FTT0007, UK). Specimens measuring 100 mm × 6.5 mm × 3.0 mm, 125 mm × 12.5 mm × 3.0 mm, and 100 mm × 100 mm × 3.0 mm were prepared for these particular tests. The measurements were executed

in accordance with ASTM D2863, ASTM D3801, and ISO 5660 guidelines, applying a heat flux of 50 kW/m² during CCT.

The microstructure of the char residue and the fracture surface of the specimens were analyzed using scanning electron microscopy (SEM, Phenom ProX, Netherlands) and X-ray photoelectron spectroscopy (XPS, Thermo EscaLab Xi+, USA).These analyses were conducted at operating voltages of 15 kV for SEM and 14.4 kV for XPS.

For the assessment of mechanical properties, a universal testing machine (MTS Systems Co., Ltd. CMT6104, China) was employed. Tests were carried out on standard dumbbell-shaped samples following the GB/T 528–2009 standard, with a test speed set at 20 mm·min⁻¹.

3. Results and discussion

3.1 Characterization of the phosphonamide flame retardants

PPDA, DAPPO, and PPNDB were synthesized by the condensation reaction of phenylphosphonic dichloride with p-phenylenediamine, aniline, and 2-aminobenzothiazole, respectively. The molecular structures of these compounds were characterized using FTIR and ¹H NMR techniques. Figure 1(a) presents the FTIR spectra for the compounds PPDA, DAPPO, and PPNDB. Notably, the characteristic absorption peaks appear at 3229 cm⁻¹, 1125 cm⁻¹, and 930 cm⁻¹, which are indicative of the stretching vibrations associated with -NH- groups, P = O bonds, and P-N bonds, respectively. Additionally, the absorption peaks observed in the spectral regions of 3100 cm⁻¹, 1500 cm⁻¹, and between 700–800 cm⁻¹ further confirm the presence of aromatic rings within these compounds. The characterization of the molecular structures of the compounds was performed utilizing FTIR and ¹H NMR methodologies. In Fig. 1 (a), the FTIR spectra for PPDA, DAPPO, and PPNDB are depicted. Notable absorption peaks appeared at 3229 cm⁻¹, 1125 cm⁻¹, and 930 cm⁻¹, which are associated with the stretching vibrations of -NH-, P = O, and P-N bonds, respectively. Additionally, the peaks observed in the ranges of 3100 cm⁻¹, 1500 cm⁻¹, and 700–800 cm⁻¹ further validate the existence of aromatic rings. All these peaks are observed in the FTIR spectra of PPDA, DAPPO, and PPNDB. In addition, the absorption peak at 1590 cm⁻¹ in the curve of PPNDB corresponds to the stretching vibration of C = N, originating from 2-aminobenzothiazole. The presence of these peaks indicates the successful synthesis of PPDA, DAPPO and PPNDB. Figure 1(b) presents the ¹H NMR spectra of PPDA, PPNDB, and DAPPO. The signals in the ¹H NMR spectra are mainly concentrated on the hydrogen atoms of the aromatic rings, appearing in the range of 8.0-6.8 ppm. The hydrogen atoms of the -NH_2 group in PPDA resonate at 6.5 ppm, while its -NH- proton appears at 6.9 ppm. For DAPPO and PPNDB, the -NH- protons are observed at 6.8 ppm and 7.1 ppm, respectively. TG and DTG curves under nitrogen revealed that the flame retardants PPDA, DAPPO, and PPNDB have initial decomposition temperatures ($T_{5\%}$, Fig. 1c) of 250°C, 234°C, and 250°C, respectively. This thermal stability falls within a suitable processing window for TPU. At 700°C, the char yields of DAPPO and PPNDB are 7.9% and 6.2%, both significantly lower than that of PPDA (36.0%).

3.2 Thermal properties of TPU composites

Figure 2. shows the TG curves of TPU composites with different loadings of PPDA, PPNDB and DAPPO. Table S1 lists the TG and DTG data of TPU, TPU/PPDA, TPU/PPNDB, and TPU/DAPPO composites under a nitrogen atmosphere. TPU undergoes a two-step degradation under nitrogen, as revealed by TGA. The initial weight loss, occurring between 220 and 320°C, results from the cleavage of hard-segment urethane bonds (-NHCOO-). This is followed by a second stage from 320 to 450°C, where weight loss takes place due to the decomposition of soft-segment polyether polyols [26–29].

After the addition of PPDA, the first-stage maximum decomposition temperature ($T_{max,1}$) of the TPU/PPDA composite was decreased slightly, while the second-stage maximum decomposition temperature ($T_{max,2}$) was increased to a small extent. This indicates that PPDA affects the decomposition of urethane bonds, leading to a decrease in the first-stage decomposition temperature [30, 31]. During the first decomposition stage, a more stable intermediate is formed via the reaction between PPDA and TPU, and consequently the second stage decomposition temperature is elevated. All TPU/PPDA composite experimental char residues exceed the calculated values, with the exception of TPU/PPDA-6. This suggests that incorporating PPDA enhances the charring process of TPU.

For TPU/PPNDB composites, both the initial decomposition temperature ($T_{d,1\%}$) and the $T_{max,1}$ of TPU are reduced, with a greater reduction observed at higher PPNDB loadings. Compared to neat TPU, the $T_{max,2}$ also decreases but shows a slight recovery trend with increasing PPNDB content. For TPU/DAPPO composites, the $T_{d,1\%}$, the $T_{max,1}$, and the $T_{max,2}$ all decrease with increasing DAPPO content. The addition of PPNDB and DAPPO does not increase the char yield of TPU at 700°C. A comparison between the experimental and theoretical char residues of TPU/PPNDB and TPU/DAPPO composites revealed that the experimental values at 700°C were lower than the calculated ones, indicating that neither PPNDB nor DAPPO promotes char formation in the TPU composites.

3.3 Flame retardancy of TPU and TPU composites

Multidimensional flame retardant performance tests were conducted on TPU/PPDA, TPU/PPNDB and TPU/DAPPO composites, including LOI, UL 94, and CCT. Figure 3 presents the vertical burning and LOI test results, together with the fitted LOI curve. Result indicates that pure TPU exhibits intense burning behavior, with continuous dripping during combustion. These high-temperature droplets can easily ignite surrounding combustible materials, significantly increasing the fire hazard index.

When the addition of PPNDB and DAPPO was both 6 wt%, TPU/PPNDB-6 (LOI = 32.4%) and TPU/DAPPO-6 (LOI = 28.1%) both passed the UL 94 V-0 rating. Although dripping occurred, the droplets did not ignite the cotton placed underneath. The melting and dripping phenomenon was alleviated in TPU composites incorporating PPDA at identical concentrations. With a loading of 9 wt% PPDA, the TPU composite demonstrated a UL 94 V-0 classification. Moreover, when the addition of PPDA in TPU composites reached 12 wt%, the UL 94 V-0 rating was achieved without any droplets, indicating a better flame retardant effect. As the content of PPDA and DAPPO gradually increased, the LOI of TPU/PPDA and

TPU/DAPPO flame retardant composites both increased progressively, with PPDA showing a better effect than DAPPO. An LOI value of 32% was reached for the TPU composite with a PPDA content of 9 wt%. In contrast, DAPPO required an addition of 12 wt% to achieve an LOI value of 32%.

The LOI of the TPU composite did not increase progressively upon the addition of PPNDB. Although an LOI value of 32% was achieved at a PPNDB content of 6 wt%, the melting and dripping phenomenon became more severe when the content exceeded 6 wt%, making it difficult to measure the LOI value in practice. The severe melting observed in the composites with PPNDB during heating may be due to the thiazole structure in PPNDB disrupting the hydrogen-bonding network in the hard segments of TPU [32].

Figure 3. LOI and UL 94 test data of TPU/PPDA, TPU/DAPPO and TPU/PPNDB composites.

The findings from the cone calorimetry tests are illustrated in Fig. 4 and detailed in Table 2. The introduction of DAPPO and PPNDB to the tested materials produced a few decreases in the PHRR. In contrast, an increase in the concentration of PPDA significantly contributed to a more pronounced reduction in PHRR. Furthermore, the incorporation of all three flame retardants collectively resulted in a noteworthy decrease in the total heat release (THR) during the combustion process. The incorporation of flame retardants significantly improved the fire performance of TPU. The TPU/PPDA-9 composite showed the greatest improvement, reducing the PHRR and THR by 58% and 28%, respectively. Reductions of 23% (PHRR) and 36% (THR) were observed for TPU/DAPPO-9, and 13% (PHRR) and 36% (THR) for TPU/PPNDB-9, relative to the pure polymer.

As the loading levels of PPDA and DAPPO increased, the residual char yield of their respective flame-retardant TPU composites showed significant enhancement. In the Table 2, the residual char of the TPU/PPDA-12 composite reached 20.3%, compared with only 8.3% for neat TPU. Similarly, the char yield of TPU/DAPPO-12 rose markedly to 17.4%, while that of TPU/PPNDB-12 exhibited a much smaller increase to only 11.9%. These results demonstrate that PPDA and DAPPO can effectively promote the char-forming ability of TPU. The superior char-forming performance of PPDA and DAPPO can be attributed to their phenyl terminal groups, which facilitate high-temperature cross-linking to form graphitic char. In addition, the amino group present in PPDA may serve as an extra cross-linking site, further promoting the development of a three-dimensional polymeric network during pyrolysis and thereby increasing the final char residue. In contrast, PPNDB, which contains thiazole terminal groups, exhibits inferior carbonization performance. This is mainly due to the cleavage of the C–N bond in PPNDB, which releases phenyl thiazole as a gaseous decomposition product, thereby reducing the amount of solid char retained in the condensed phase [33, 34]. Simultaneously, the average effective heat of combustion (av EHC) showed a gradual decline as the loadings of DAPPO and PPNDB increased, suggesting that both additives successfully diminished the concentration of combustible gases present in the volatiles.

Table 2
Typical data from cone calorimetry testing.

Samples	TTI(s)	PHRR (kW/m^2)	THR (MJ/m^2)	av-EHC (MJ/kg)	TSR (m^2/m^2)	R_{350s} (%)
TPU	40	1388	86	22.0	1664	8.3
TPU/PPDA-3	35	1318	75	21.0	2172	12.3
TPU/PPDA-6	33	1068	70	23.3	2237	12.1
TPU/PPDA-9	36	586	61	21.8	2371	13.4
TPU/PPDA-12	30	497	59	22.1	2059	20.3
TPU/DAPPO-3	31	1712	67	18.0	1410	11.0
TPU/DAPPO-6	29	853	54	15.1	1384	14.6
TPU/DAPPO-9	25	1068	52	14.9	1454	16.4
TPU/DAPPO-12	27	1095	56	13.6	1762	17.4
TPU/PPNDB-3	31	1028	78	21.5	2121	10.8
TPU/PPNDB-6	30	1454	79	21.7	2210	8.0
TPU/PPNDB-9	24	1121	71	20.0	2175	10.2
TPU/PPNDB-12	25	1096	68	19.2	2326	11.9

3.4 Residual char analysis of TPU and TPU composites

The flame retardant effectiveness in the condensed phase can be inferred from the structure and morphology of the post-combustion char. Therefore, an analysis of the residual chars obtained from cone calorimetry was conducted. The resulting macro- and micro-morphological images for TPU/PPDA-9, TPU/DAPPO-9 and TPU/PPNDB-9 composites are shown in Fig. 5. Figure $5b_1$ revealed that the residual char of pure TPU was observed to be thin (0.5 cm) with large cracks in certain areas, which resulted in the exposure of the underlying aluminium foil. In contrast, the TPU/DAPPO-9 and TPU/PPDA-9 systems formed continuous intumescent char layers with thicknesses of 1.2 cm and 1.5 cm, respectively. The residual char layer of TPU/PPNDB-9 was slightly increased in height (0.7 cm) with a slight increase in char yield but still exhibited large pores on the surface.

In the SEM images of the residual char after cone calorimetry testing shown in Fig. 5 (c1-c4), a dense and intact char layer was observed for TPU/PPDA-9, and the residual char of TPU/DAPPO-9 and TPU/PPNDB-9 had significantly more pores than that of TPU/PPDA-9. Moreover, the residual char surfaces of both TPU/DAPPO-9 and TPU/PPNDB-9 were porous, which could be attributed to the escape of gas-phase products generated during combustion. Notably, the pores on the TPU/DAPPO-9 surface exhibited an irregular morphology, with some being partially closed or non-penetrating. In contrast, the

pores on the TPU/PPNDB-9 char surface appeared predominantly circular. This distinct pore structure implies that the char layer of TPU/DAPPO-9 possessed higher strength than that of TPU/PPNDB-9.

To investigate the surface chemical states, XPS analysis was performed on the residual chars of pure TPU, TPU/PPDA-9, TPU/DAPPO-9, and TPU/PPNDB-9 after CCT. As summarized in Fig. 6 and Table 3, the spectrum exhibits three peaks at 284.8 eV, 285.8 eV, and 289.1 eV, which are assignable to C-C, C-O, and C = O, respectively. The degree of oxidation of the char layer can be inferred from the relative areas of these characteristic peaks. Specifically, a more robust char layer is indicated by a higher proportion of C-C bonds relative to the oxidized C-O and C = O bonds. In comparison to pure TPU, a favorable spectral signature was observed in all TPU composites: a reduction in the C-O and C = O peak areas alongside an increase in the C-C peak area. Moreover, the C-C peak area was higher for TPU/PPDA-9 (75.8%) and TPU/DAPPO-9 (74.2%) than for TPU/PPNDB-9 (68.5%). This indicates that incorporating PPDA and DAPPO contributes positively to the development of a more robust char layer within the TPU matrix, thereby enhancing the condensed-phase flame retardant effect of the TPU matrix [15, 21].

As indicated in Table 3, phosphorus originating from all three flame retardant additives was incorporated into the char. The measured phosphorus contents were 0.5% for TPU/PPDA-9, 1.2% for TPU/DAPPO-9, and 1.3% for TPU/PPNDB-9 in the residual chars.

Table 3
Elemental composition of the residual char of TPU, TPU/DAPPO-9, TPU/PPDA-9, and TPU/PPNDB-9 after cone calorimetry testing.

Element of char (%)	C	O	N	P
TPU	83.5	8.7	7.8	0
TPU/PPDA-9	84.2	8.0	7.3	0.5
TPU/DAPPO-9	79.4	10.4	9.0	1.2
TPU/PPNDB-9	76.5	11.3	10.9	1.3

3.5 Mechanical properties of TPU and TPU composites

Figure 7(a) and (b) depict the relative tensile strength and relative elongation at break, respectively, which were calculated using the following formulas:

As shown in Fig. 7(a), with the increasing content of flame retardant, the tensile strength of TPU composites continuously decreased. TPU composites containing PPDA and DAPPO retained their tensile strength better than those containing PPNDB. Compared to pure TPU, the tensile strength retention rates of TPU/PPDA-3 and TPU/DAPPO-3 composites were 54.2% and 46.1%, respectively, higher than that of TPU/PPNDB-3 composite (29.4%). At this time, the elongation at break retention rates of TPU/PPDA-3 and TPU/DAPPO-3 composites were 71.5% and 64.9%, respectively, while the elongation at break of TPU/PPNDB-3 decreased to 43.8%.

Figure 7(c-f) show the SEM images of the fracture surfaces of TPU, TPU/PPDA-3, TPU/DAPPO-3 and TPU/PPNDB-3 composites after tensile testing. In contrast to the fracture surface of TPU/PPDA-3, particles of the flame retardant could be observed on the fracture surface of TPU/DAPPO-3. The poor compatibility observed in the TPU/DAPPO system accounts for its less favorable mechanical performance when compared to the TPU/PPDA composite.

4. Conclusions

In this study, the influence of the terminal groups of the phosphonamide flame retardants on the properties of flame retarded TPU was investigated. The results showed that at the same loading, the amino-terminated PPDA and phenyl-terminated DAPPO exhibited superior flame retardancy compared to PPNDB with a thiazole terminal group. Under the same loading conditions, the LOI for the TPU composite containing PPDA exceeded that of the composite with DAPPO. Incorporating 6 wt% DAPPO allowed the TPU composite to attain a UL 94 V-0 classification, whereas a requirement of 9 wt% PPDA was necessary to reach the same level. The addition of 12 wt% PPDA to TPU suppressed melt dripping. In the case of PPNDB (with thiazole terminal groups), a LOI of 32% and a UL 94 V-0 rating are achieved at a 6 wt% addition level. However, severe melting is exhibited by the material upon heating, negatively impacting its application and testing. Cone calorimetry revealed that TPU/PPDA-9 exhibited the greatest reduction in PHRR relative to neat TPU, by 58%. The PHRR of the TPU/DAPPO-9 and TPU/PPNDB-9 composites was reduced by 23% and 13%, respectively. Thermogravimetric analysis, morphology of the char layer, and XPS test results indicated that the char-forming ability promoted by PPDA was higher than that of DAPPO and PPNDB. This phenomenon was linked to the aminophenyl group present in PPDA, which has the capability to induce dehydration and cross-linking of TPU under elevated temperatures, resulting in the creation of a dense, intumescent char layer. Furthermore, the test results of mechanical properties showed that at a 3 wt% loading, the retention of tensile strength (54%) and the retention of elongation at break (72%) for the TPU/PPDA-3 system were better than those for the TPU/DAPPO-3 and TPU/PPNDB-3 systems.

Declarations

Supplementary Information

The online version contains supplementary material available at .

Acknowledgements

This work was financially supported by National Natural Science Foundation of China (Grant No. 22175006).

Author contributions

Kai Wei: Writing–original draft, Writing–review and editing, Data curation and Visualization, **Yingxin Li**: Writing–original draft, Investigation and Validation. **Yajun Chen**: Writing– review & editing and Supervision.

Funding

This work was financially supported by National Natural Science Foundation of China (Grant No. 22175006).

Data availability

Data will be made available on request.

The authors declare that they have no known competing financial interests or personal relationships that could have appeared to influence the work reported in this paper.

References

1. Shi C, Wan M, Duan J, Qian X, Che H, Li J, Ren F, Li J, Yang L (2024) Core-shell flame retardants based on Chitosan@MMT coated ammonia polyphosphate for enhancing flame retardancy of polyurethane, Compos. Part A Appl. Sci Manuf 176:107831. https://doi.org/10.1016/j.compositesa.2023.107831
2. Xia Y, Zhang X, An L, Xie Y, Wu F, Mei Y, Xie D, Feng D (2025) Synergistic flame retardancy of cross-linked kraft lignin and black phosphorus on TPU: Mechanism and performance. Chem Eng J 519:165178. https://doi.org/10.1016/j.cej.2025.165178
3. Gama NV, Ferreira A, Barros-Timmons A (2018) Polyurethane foams: Past, present, and future. Materials 11:1841. https://doi.org/10.3390/ma11101841
4. Hu J, Peng J, Tian J, Xiao C (2023) Thermal performance of thermoplastic polyurethane composites with microencapsulated piperazine pyrophosphate. Front Mater 10:1178475. https://doi.org/10.3389/fmats.2023.1178475
5. Khalifa M, Anandhan S, Wuzella G, Lammer H, Mahendran AR (2020) Thermoplastic polyurethane composites reinforced with renewable and sustainable fillers – a review. Polym Plast Technol Mater 59:1751–1769. https://doi.org/10.1080/25740881.2020.1768544
6. Wu J, Zhang X, Qin Z, Zhang W, Yang R (2023) Inorganic/organic phosphorus-based flame retardants synergistic flame retardant rigid polyurethane foam. Polym Eng Sci 63(3):1041–1049. https://doi.org/10.1002/pen.26264
7. Gang Y, Xu Y, Qin A, Li Q, Yan C, Zhang W, Xu M, Xu K, Li B, Liu L (2024) Design, construction and mechanism of highly efficient flame retardant, UV shielding and transparent thermoplastic polyurethanes. Chem Eng J 500:157446. https://doi.org/10.1016/j.cej.2024.157446
8. Li D, Liu L, Zhang Z, Xu M, Xu Y, Qian L (2021) An urethane-based phosphonate ester for improving flame retardancy and smoke suppression of thermoplastic polyurethane. Polym Degrad Stab

188:109568. https://doi.org/10.1016/j.polymdegradstab.2021.109568

9. Lin M, Li B, Li Q, Li S, Zhang S (2011) Synergistic effect of metal oxides on the flame retardancy and thermal degradation of novel intumescent flame-retardant thermoplastic polyurethanes. J Appl Polym Sci 121(4):1951–1960. https://doi.org/10.1002/app.33759
10. Sun Z, Chen Y, Tang W, Qiu Y, Qian L (2023) Strategies for simultaneously improving the mechanical properties and flame retardancy of TPU through hydrogen bonding. J Therm Anal Calorim 148:9843–9855. https://doi.org/10.1007/s10973-023-12351-6
11. Chen X, Ma C, Jiao C (2016) Enhancement of flame-retardant performance of thermoplastic polyurethane with the incorporation of aluminum hypophosphite and iron-graphene. Polym Degrad Stab 129:275–285. https://doi.org/10.1016/j.polymdegradstab.2016.04.017
12. Huang Y, Jiang S, Liang R, Liao Z, You G (2019) A green highly-effective surface flame-retardant strategy for rigid polyurethane foam: Transforming UV-cured coating into intumescent self-extinguishing layer. Compos Part Appl Sci Manuf 125:105534. https://doi.org/10.1016/j.compositesa.2019.105534
13. Wan L, Deng C, Chen H, Zhao Z-Y, Huang S-C, Wei W-C, Yang A-H, Zhao H-B, Wang Y-Z (2021) Flame-retarded thermoplastic polyurethane elastomer: From organic materials to nanocomposites and new prospects. Chem Eng J 417:129314. https://doi.org/10.1016/j.cej.2021.129314
14. Liu C, Shi Y, Feng Y, You X, Xie W, Ke Y, Wang H, Chen L, Wang Y (2022) Design of core-multi shell flame retardant towards fire safe thermoplastic polyurethane composites with low toxic fumes generation. Compos Commun 35:101339. https://doi.org/10.1016/j.coco.2022.101339
15. Xin H, Chen Y, Li X, Li Y, Peng Q, Luo H (2023) Fabrication of inorganic coatings incorporated with phosphorus-nitrogen-functionalized graphene oxide nanosheets to improve waterborne polyurethanes fire retardancy. Polym Test 128:108219. https://doi.org/10.1016/j.polymertesting.2023.108219
16. Li M, Chen C, Hai W, Jiang Z, Meng Q, Hao E, Li H, Shao H, Shao G, Jiang J, Chen N, Bi S (2024) Investigation of MXene@APP/FDS/AgNPs@EG system for preparing multifunctional thermoplastic polyurethane composites with flame retardancy and electromagnetic shielding performance. Compos Part Appl Sci Manuf 186:108409. https://doi.org/10.1016/j.compositesa.2024.108409
17. Chen Y, Peng H, Li J, Xia Z, Tan H (2014) A novel flame retardant containing phosphorus, nitrogen, and sulfur: Synthesis and application in thermoplastic polyurethane. J Therm Anal Calorim 115:1639–1649. https://doi.org/10.1007/s10973-013-3461-0
18. Liu L, Xu Y, He Y, Xu M, Shi Z, Hu H, Yang Z, Li B (2019) An effective mono-component intumescent flame retardant for the enhancement of water resistance and fire safety of thermoplastic polyurethane composites. Polym Degrad Stab 167:146–156. https://doi.org/10.1016/j.polymdegradstab.2019.07.006
19. Hao F, Chen Y, Han L, Qian L (2024) Elemental synergy flame retardant effect of Schiff base derivatives with similar chemical structure in TPU. Mater Today Commun 40:109983. https://doi.org/10.1016/j.mtcomm.2024.109983

20. Yang A, Deng C, Chen H, Wei Y, Wang Y (2017) A novel Schiff-base polyphosphate ester: Highly-efficient flame retardant for polyurethane elastomer. Polym Degrad Stab 144:70–82. https://doi.org/10.1016/j.polymdegradstab.2017.08.007
21. Li M, Hao F, Chen Y, Qian L (2023) Facile alteration of the molecular structure of phosphonamide for efficient flame retardancy in TPU. Compos Commun 44:101759. https://doi.org/10.1016/j.coco.2023.101759
22. Jian R, Ai Y, Xia L, Zhao L, Zhao H (2019) Single component phosphamide-based intumescent flame retardant with potential reactivity towards low flammability and smoke epoxy resins. J Hazard Mater 371:529–539. https://doi.org/10.1016/j.jhazmat.2019.03.045
23. Chen H, Deng C, Zhao Z (2020) Novel piperazine-containing oligomer as flame retardant and crystallization induction additive for thermoplastics polyurethane. Chem Eng J 400:125941. https://doi.org/10.1016/j.cej.2020.125941
24. Li M, Chen Y, Kong Z (2023) Impact of a novel phosphoramide flame retardant on the fire behavior and transparency of thermoplastic polyurethane elastomers. ACS Omega 8:18358–18371. https://doi.org/10.1021/acsomega.3c01464
25. Shi H, Chen Y, Hao F (2025) Polymer-based phosphoramidite flame retardant for TPU: Enhanced fire resistance with preserved transparency and mechanical properties. Polym Degrad Stab 232:111103. https://doi.org/10.1016/j.polymdegradstab.2024.111103
26. Zhang W, Xu Y, Yan C, Gang Y, Qin A, Xu K, Xu M, Li B, Liu L (2024) Preparation of novel and efficient arylphosphonate flame retardants for simultaneously enhancement of fire safety and UV-shielding properties of transparent thermoplastic polyurethane. Polym Degrad Stab 230:111029. https://doi.org/10.1016/j.polymdegradstab.2024.111029
27. Li H, Ning N, Zhang L, Wang Y, Liang W, Tian M, Chan T (2015) Effect of content of organophosphorus on flame retardancy mode of thermoplastic polyurethane. Polymer 67:1–11. https://doi.org/10.1016/j.polymer.2015.04.027
28. Zeller M, Garbev K, Weigel L, Saatzer T, Merz D, Tavakkol S, Stapf D (2023) Thermogravimetric studies, kinetic modeling and product analysis of the pyrolysis of model polymers for technical polyurethane applications. J Anal Appl Pyrol 171:105976. https://doi.org/10.1016/j.jaap.2023.105976
29. Hong N, Liu J, Gao L, Wu Z, Huang Y, Zhang L, Wang X, Sun J (2024) Novel polysilazane microencapsulated ammonium polyphosphate as flame retardant and smoke suppressant for thermoplastic polyurethane. Polym Bull 81:16557–16573. https://doi.org/10.1007/s00289-024-05479-4
30. Ye T, Li Y, Chen Y, Qian L (2025) Molecular structure-dependent flame retardancy of phosphonamides in thermoplastic polyurethane elastomer: Aliphatic chains vs aromatic rings. ACS Appl Polym Mater 7:13478–13487. https://doi.org/10.1021/acsapm.5c02053
31. Li Y, Chen Y, Ye T, Han L, Hao J, Qian L (2025) Enhancing flame retardancy of thermoplastic polyurethane elastomers: The role of phosphonamide molecular weight. Eur Polym J 236:114158.

https://doi.org/10.1016/j.eurpolymj.2025.114158

32. Allami T, Alamiery A, Nassir M, Kadhum A (2021) Investigating physio-thermo-mechanical properties of polyurethane and thermoplastics nanocomposite in various applications. Polymers 13:2467. https://doi.org/10.3390/polym13152467
33. Zhang Q, Yang S, Wang J, Cheng J, Zhang Q, Ding G, Hu Y (2019) A DOPO based reactive flame retardant constructed by multiple heteroaromatic groups and its application on epoxy resin: Curing behavior, thermal degradation and flame retardancy. Polym Degrad Stab 167:10–20. https://doi.org/10.1016/j.polymdegradstab.2019.06.020
34. Mountassir A, Tirri T, Sund P, Wilén C (2021) Sulfenamides as standalone flame retardants for polystyrene. Polym Degrad Stab 188:109588. https://doi.org/10.1016/j.polymdegradstab.2021.109588

Scheme 1

Scheme 1 is available in the Supplementary Files section.

Figures

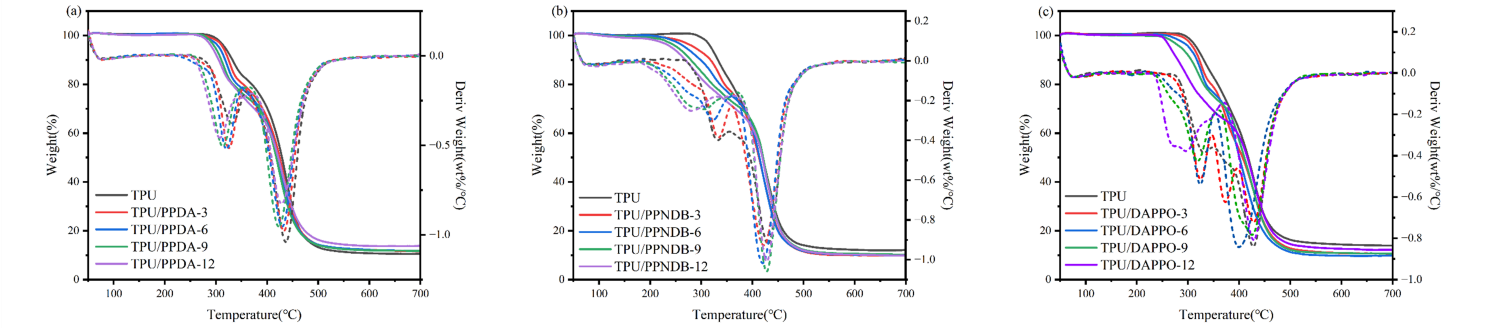


Figure 1

FTIR spectra of PPDA, DAPPO, and PPNDB (a); ¹H NMR spectra (b); TG and DTG curve(c).

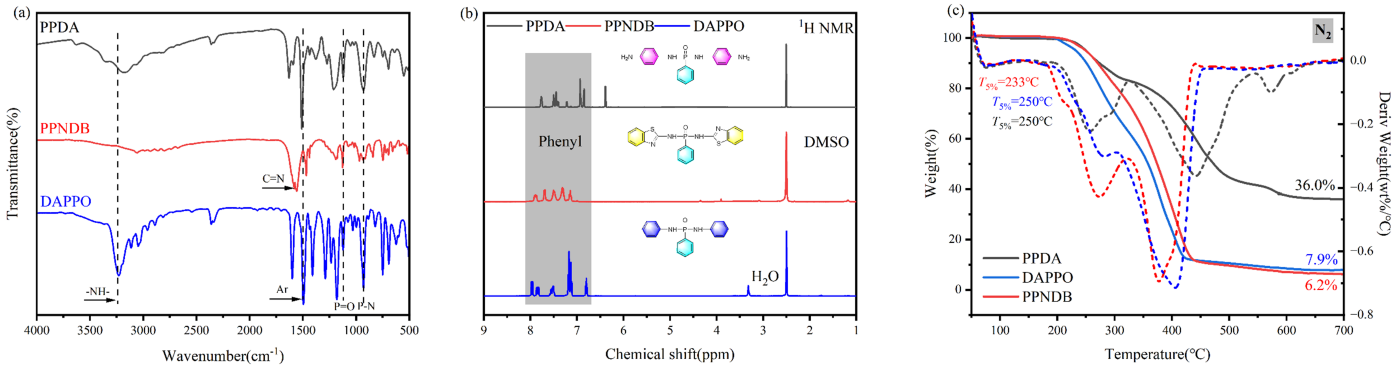


Figure 2

TG and DTG curves of TPU, TPU/PPDA composites(a), TPU/DAPPO composites (b), and TPU/PPNDB composites (c) under a nitrogen (N_2) atmosphere.

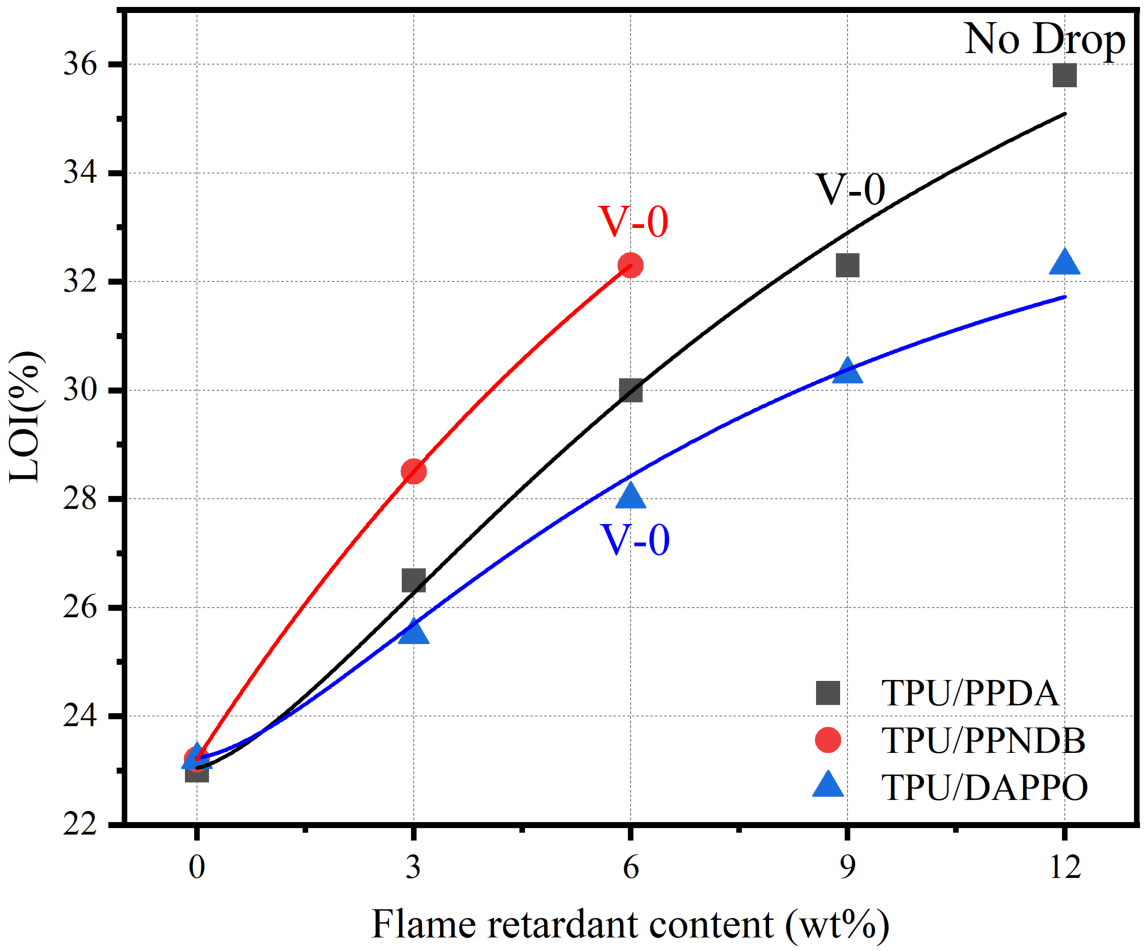


Figure 3

LOI and UL 94 test data of TPU/PPDA, TPU/DAPPO and TPU/PPNDB composites.

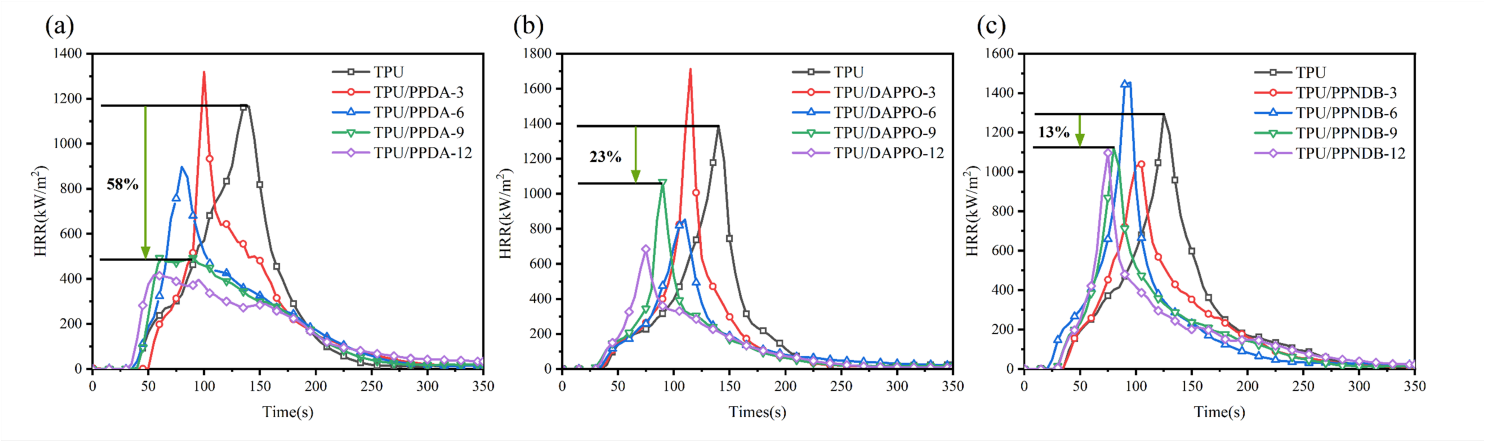


Figure 4

HRR curves of TPU, TPU/PPDA (a), TPU/DAPPO (b), and TPU/PPNDB (c) composites.

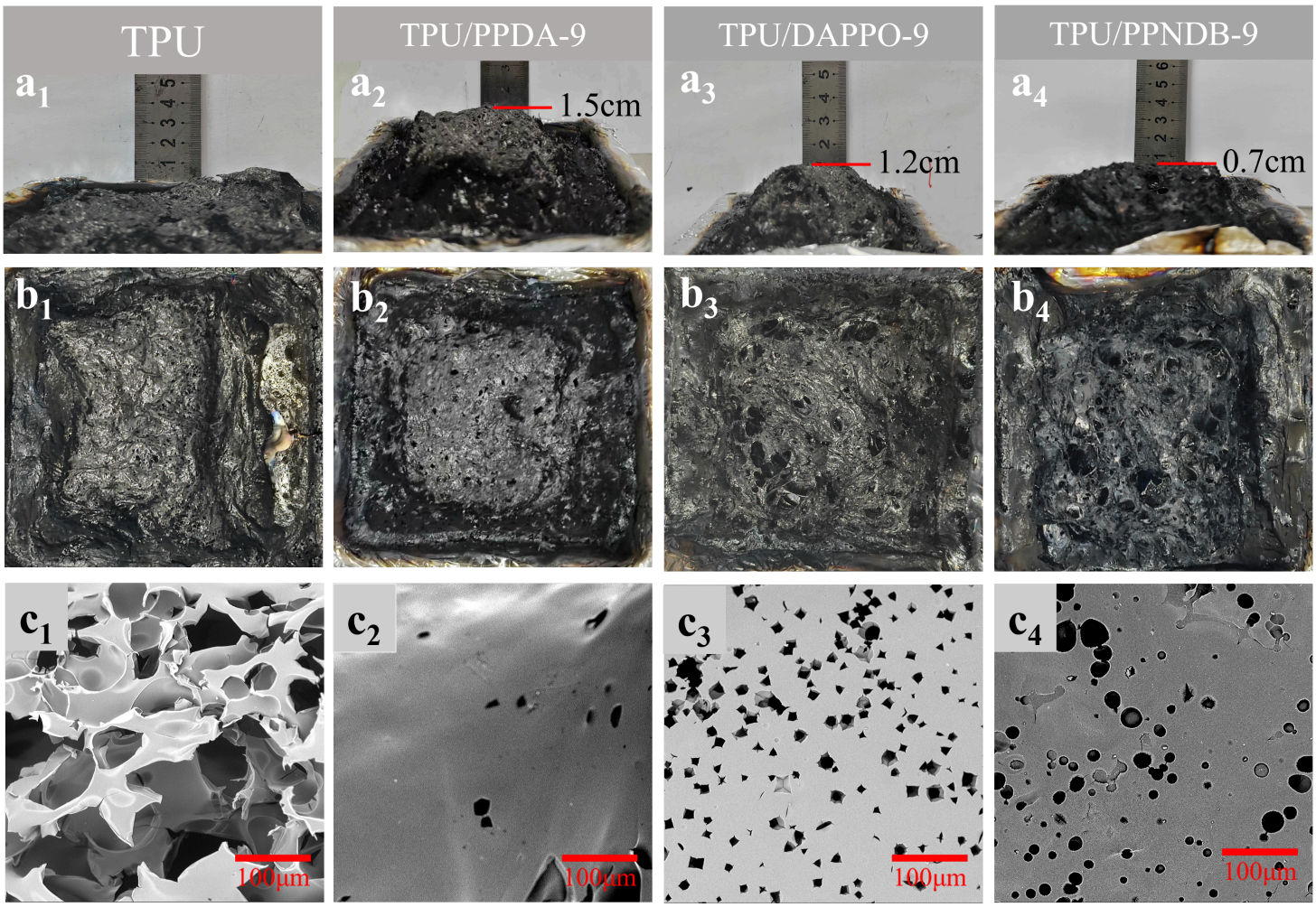


Figure 5

Macroscopic and microscopic images of the residual char of TPU, TPU/PPDA-9, TPU/DAPPO-9, TPU/PPDA-9, and TPU/PPNDB-9 composites after cone calorimetry testing.

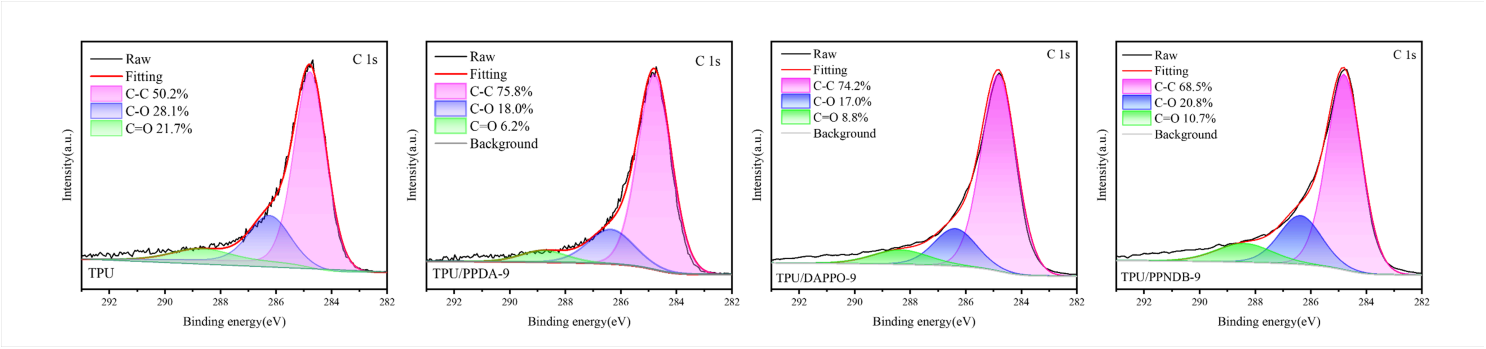


Figure 6

XPS spectra of TPU (a), TPU/PPDA-9 (b), TPU/DAPPO-9 (c), and TPU/PPNDB-9 (d).

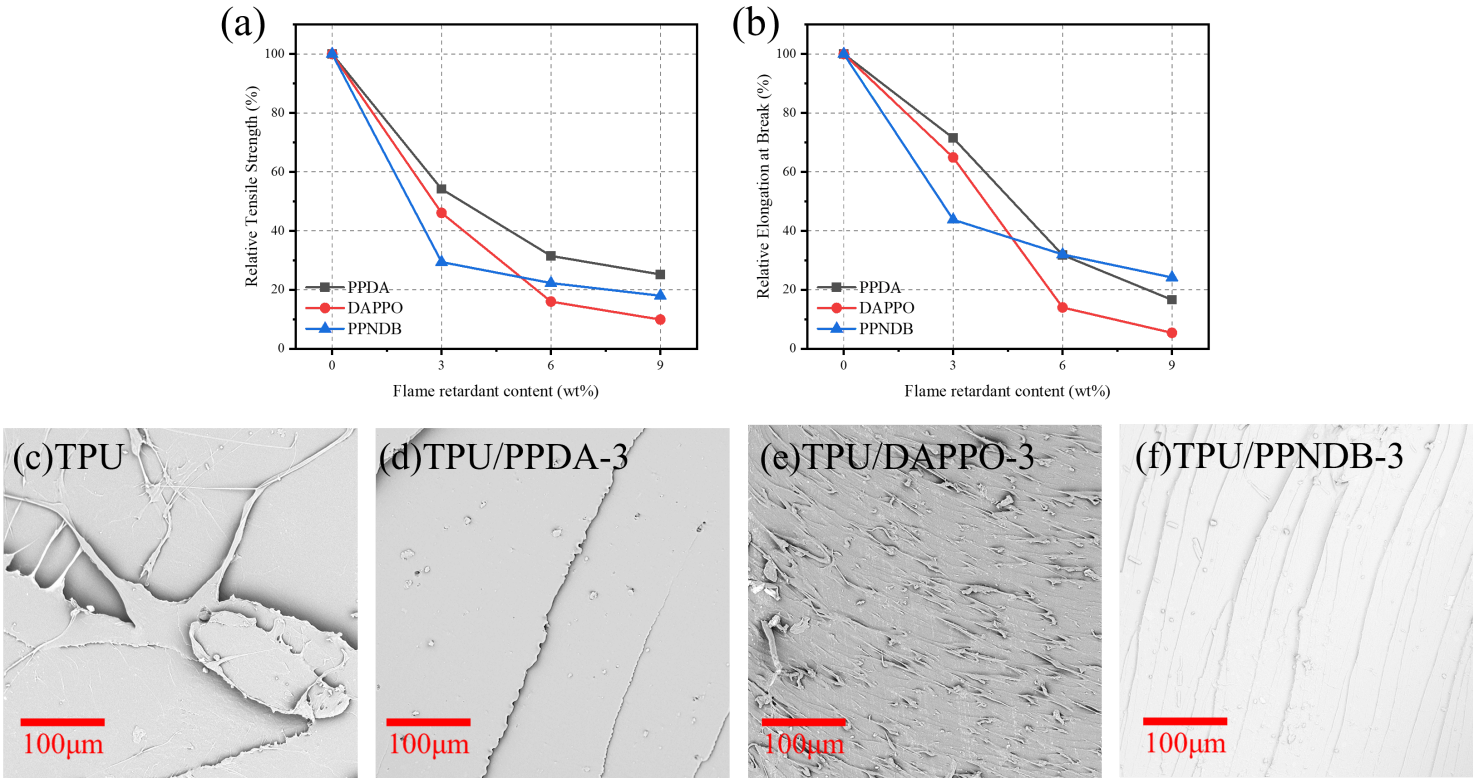


Figure 7

Tensile testing results of TPU, TPU/DAPPO, and TPU/PPNDB composites (a, b), and SEM images of the tensile fracture surfaces of TPU (c), TPU/PPDA-3 (d), TPU/DAPPO-3 (e), and TPU/PPNDB-3 (f) composites.

Supplementary Files

This is a list of supplementary files associated with this preprint. Click to download.

- Scheme1.png

- SupplementaryMaterial.docx